HHS Public Access

Author manuscript

J Neurol Neurosurg Psychiatry. Author manuscript; available in PMC 2020 June 16.

Published in final edited form as:

J Neurol Neurosurg Psychiatry. 2020 May ; 91(5): 533–539. doi:10.1136/jnnp-2019-321973.

Differentiating Tic Electrophysiology from Voluntary Movement in the Human Thalamocortical Circuit

Jackson Cagle, M. S.[1,Ψ], **Michael S. Okun, M.D.**[2,Ψ], **Enrico Opri**[1], **Stephanie Cernera**[1], **Rene Molina**[3], **Kelly Foote, M. D.**[4], **Aysegul Gunduz, Ph.D.**[1,2,*]

[1]Department of Biomedical Engineering, University of Florida, Gainesville FL

[2]Department of Neurology, Fixel Institute for Neurological Diseases, University of Florida, Gainesville, FL

[3]Department of Electrical and Computer Engineering, University of Florida, Gainesville FL

[4]Department of Neurosurgery, Fixel Institute for Neurological Diseases, University of Florida, Gainesville, FL

Abstract

Objectives—Tourette syndrome is a neurodevelopmental disorder commonly associated with involuntary movements, or tics. We currently lack an ideal animal model for Tourette syndrome. In humans, clinical manifestation of tics cannot be captured via functional imaging due to motion artifacts and limited temporal resolution, and electrophysiological studies have been limited to the intraoperative environment. The goal of this study was to identify electrophysiological signals in the centromedian (CM) thalamic nucleus and primary motor (M1) cortex that differentiate tics from voluntary movements.

Methods—The data was collected as part of a larger NIH sponsored clinical trial. Four participants (2 males, 2 females) underwent monthly clinical visits for collection of physiology for a total of six months. Participants were implanted with bilateral CM thalamic macroelectrodes and M1 subdural electrodes that were connected to two neurostimulators, both with sensing capabilities. MRI scans were performed pre-operatively and CT scans post-operatively for localization of electrodes. Electrophysiological recordings were collected at each visit from both the cortical and subcortical implants.

Results—Recordings collected from the CM thalamic nucleus revealed a low-frequency power (3-10 Hz) increase that was time-locked to the onset of involuntary tics but was not present during

*Corresponding Author: Aysegul Gunduz, Ph.D., agunduz@ufl.edu, Mailing Address: University of Florida, PO Box 116131, Gainesville, FL 32611.

ΨCo-First Authors

Contributorship Statement

JNC: Collected data, performed data analysis, wrote first draft
MSO: Designed and clinically supervised study, edited manuscript
KF: Performed surgical implantation, edited manuscript
AG: Designed and supervised study, edited manuscript

Competing Interests

The authors report no competing interests.

voluntary movements. Cortical recordings revealed beta power decrease in M1 that was present during tics and voluntary movements.

Conclusion—We conclude that a human physiological signal was detected from the centromedian thalamus that differentiated tic from voluntary movement, and this physiological feature could potentially guide the development of neuromodulation therapies for Tourette syndrome that could utilize a closed-loop based approach.

Keywords

Tourette syndrome; tics; deep brain stimulation; DBS; electrophysiology; centromedian thalamus; motor cortex

Introduction

Tourette syndrome (TS) is a chronic neurodevelopmental disorder characterized by motor and phonic tics[1]. TS is commonly associated with other neuropsychiatric comorbidities (e.g., attention deficit hyperactivity disorder (ADHD), obsessive compulsive features (OCD), and other behavioral manifestations). For a majority of TS cases, motor manifestations can be managed using a combination of medications [2,3], and behavioral therapies (i.e. comprehensive behavioral intervention for tics (CBIT)) [4,5]. The expected progression of TS would anticipate that most patients will experience significant improvements of tics in late adolescence or early adulthood. However, experts now recognize that there is a subset of patients who will continue to experience disabling tics despite optimal medication and behavioral management. For these severely affected patients, deep brain stimulation (DBS) has been recently applied to address refractory and disabling tics.

Over the past two decades, DBS has been used as a promising treatment option for medication refractory and severely affected TS patients [6–8]. Evidence from neuroimaging [9–11], stereotactic lesions [12–14], and animal models [15–17] have collectively demonstrated that the thalamo-striatal-cortical circuit [18] is involved in the pathophysiology of TS. Based on these findings, thalamic and pallidal nuclei in the circuits have been selected as DBS targets for treatment of TS. Although multiple brain targets have been targeted for the treatment of tics, we chose the centromedian (CM) thalamic nucleus because it is the most widely published TS DBS target with promising outcomes worldwide [6]. Intraoperative electrophysiological recordings of CM thalamic nucleus from our group and others have revealed that pathological low-frequency activity was correlated with tic severity [19–21]. Our a priori hypothesis was that network physiology recorded from the CM thalamic nucleus and the primary motor (M1) cortex could be used to differentiate tic from voluntary movement. This study captured the physiology of tic in awake behaving humans. Unique to this study from previous TS physiological recordings was the use of chronically implanted depth and surface electrocorticogram (ECoG) recording and stimulation devices, which captured chronic real time local field potentials (LFPs) from the CM thalamic nucleus and M1 cortex [22].

Methods

Participants

This study was approved by both the Institutional Review Board (IRB) of the University of Florida (UF) and the U.S. Food and Drug Administration (FDA) through an Investigational Device Exemption (IDE). Patients with medication refractory TS were screened, consented and enrolled into the study at UF Fixel Institute for Neurological Diseases. All patients were consented as according to the Declaration of Helskinki and the written consent form was approved by the local ethical committee. The study was registered at clinicaltrials.gov (NCT02056873) with detailed inclusion/exclusion criteria: A DSM-V diagnosis of TS, Yale Global Tic Severity Scales (YGTSS) of >35/50 for at least 12 months, and a motor tic subscore >15 [23]. The TS diagnosis was required to cause incapacitation with severe distress, self-injurious behavior, and/or quality of life disruption. OCD, depression, and ADHD were not exclusionary criteria provided the tics were the major issue prompting potential surgical intervention. Subjects were required to have trials of at least three dopamine blocking drugs and a minimum of a single trial with an alpha-2 adrenergic agonist. Subjects were required to be on stable doses of TS medications throughout the trial. Subjects with unstable psychiatric disorders were excluded.

Surgical Procedure

Subjects enrolled in the study underwent two stages of stereotactic surgical intervention [24]. The first stage was performed awake and the surgeon implanted bilateral depth electrodes in the CM thalamic region and subdural ECoG strips over the hand motor cortex. The second stage of the operation was performed approximately 30 days following the first stage and was used to implant the bidirectional Activa PC+S neurostimulator (Medtronic PLC, Minneapolis, MN). Medtronic Model 3387 DBS leads were implanted bilaterally in CM nuclei, each with 4 1.5mm contacts and 3.0 mm center-to-center spacing. The electrode target trajectories into the CM nuclei were identified using direct visualization and manipulation of a modified digital Schaltenbrand-Bailey atlas [25]. The atlas was morphed onto the pre-operative magnetic resonance imaging (MRI) FGATIR image [26] and the co-registered pre-operative computed tomography image (CT) was used as a reference. Microelectrode recordings were performed to confirm the target area. Medtronic RESUME II Model 3587A 4-contact subdural strips with 4.0 mm diameter and 10.0 mm center-to-center distances were placed over the hand M1 region using real-time functional mapping of local high broadband activity (70-110Hz)[27]. During the second stage surgery, two Medtronic Activa PC+S neurostimulators were implanted bilaterally under the skin in the subclavicular region. Each neurostimulator was connected to one depth electrode and one subdural strip each implanted in the ipsilateral hemisphere.

Postsurgical Visits and Behavioral Tasks

During six monthly post-surgical visits, subjects participated in behavioral tasks, and recordings were separated into three conditions: tic suppression, voluntary movements, and tics (Figure 1). The subjects were instructed to suppress tics to their best ability for 4 minutes. Any unsuppressed tics were removed from analysis. Next, subjects were instructed to voluntarily move body parts most inflicted by severe tics repetitively for 10 seconds and

to rest for 10 seconds. Finally, the subjects were instructed to freely tic for 4 minutes [21]. Previous studies have shown that active tic suppression conditions may not be representative of the default state of the brain [28], therefore, segments of tic-free periods during tic recordings were selected as the baseline for comparison.

Data Recordings

Local field potentials (LFPs) from the CM thalamic nuclei and M1 cortex were recorded using the Activa PC+S with a bipolar recording configuration. LFPs were recorded with a sampling rate of 422Hz during three task conditions. A second set of resting state data was recorded with a sampling rate of 800Hz to perform phase-amplitude coupling analysis. The bipolar configuration was setup such that one bipolar subdural strip contact was in direct contact with M1 cortex and one bipolar depth contact was within the CM thalamic nucleus. The second reference contact was located 2 contacts away to improve the signal-to-noise ratio. The thalamic contact pair was selected by enclosing the optimal therapeutic stimulation contact with the sensing contacts (i.e., if the best treatment was found by monopolar stimulation at E01 location, recording was done with E00-E02 contact pairs). Motor tic kinematics were recorded using 8 wireless electromyographic (EMG) sensors embedded with inertia sensors (Delsys Inc., Natick, MA). Eight EMG sensors were placed symmetrically over the upper extremities of the patient. Sensors were selected to include areas with the most perceptible motor and phonic tics. Videotaping was concurrently used with kinematic recordings for labeling of motor and vocal tics collected during behavioral tasks. The Activa PC+S recordings were aligned with the kinematic recordings as follows. A 5-second long 5Hz pulse train was delivered to the CM at the beginning of each recording session, which can be detected from thalamic recordings, as well as from a wireless EMG sensor was placed on the patient's neck (over the implanted connector cable). This pulse train allowed us to align signals from two systems. Additionally, we synchronized video recordings to the EMG system by delivering a pulse train from a microcontroller to the EMG base station and a light emitting diode (LED) placed in front of the camera.

Data Analysis and Statistical Testing

LFP recordings were processed offline using MATLAB (Cambridge, MA). A 3rd-order infinite impulse response (IIR) band-pass filter between 1Hz and 100Hz was implemented to remove DC offset and high-frequency noise. Videotapes were blindly rated by movement disorders neurologists for tic labeling. If unsuppressed tics were identified during baseline recordings, the segment of data 1 second before the tic and 3 seconds after the tic were removed from analysis. If tics were identified in tic recordings, 1 second before the tic and 3 seconds after the tic were segmented into epochs for analysis of tic physiology. The tics selected for the analysis include both simple tics and complex tics, motor tics and vocal tics.

Spectrograms of tic epochs drawn from the M1 cortex and the CM thalamic nuclei were computed using the maximum entropy method (MEM) with a 500ms window and 50% overlap with a model order of 30 [29]. Afterward, the tic spectrograms were transformed to unit of decibel by log-scale transformation. The baseline spectrograms were computed using tic-free periods during tic recordings with an identical MEM setting as the tic spectrogram and these were transformed into decibel. Tic spectrograms were referenced to baseline by

subtracting the average baseline power spectral density (PSD), which was calculated by averaging baseline spectrograms across time. To address potential bias due to movement execution, spectrograms of voluntary movements were computed similarly, with the onset programmed to the onset of the voluntary movement.

The group-level tic feature was computed by averaging the tic spectrograms for all four patients in both the CM thalamic nuclei and M1 cortex. Statistical tests were performed on the group-level average tic spectrograms to identify significant features of tic onset. Two-sided student's t-tests were computed for each time-frequency pair against baseline, and the significance values were corrected for multiple comparison using false discovery rate (FDR) [30].

Data Availability

The electrophysiological data and imaging data used in the paper are available from the corresponding author upon reasonable request. Electrophysiological analysis were performed using the maximum entropy method provided by BCI2000 package [31], and imaging analysis was done using the FreeSurfer package [32].

Results

Electrophysiology and Functional Mapping

Table 1 summarizes the subjects' baseline characteristics. Four subjects were implanted and studied (2 males, 2 females) with an average age of 35.8 ± 4.1 (mean ± standard error), mean baseline YGTSS Total Tic Score (TTS) of 42.8 ±1.1, and mean disease duration of 21.8 ± 8.3. All 4 subjects completed 6 months of post-operative visits. There were no serious unexpected adverse events or surgical complications. The final optimal therapeutic stimulation settings have been summarized in Table 1. The thalamic region-of-interest was selected based on the optimal stimulation location identified by the DBS programmer who was optimizing the patient to reduce the motor and vocal tics. The raw electrophysiological characteristics of neuronal activity recorded from the subdural strips and depth electrodes prior to signal processing is summarized in Figure 2. The subdural strips revealed higher frequency activity and larger amplitude while the depth electrodes showed predominantly slow wave activity and lower amplitude (Figure 2A). Due to device memory failure in Subject 04's left Activa PC+S system, no physiology recordings were available from the left hemisphere. The root mean square (RMS) amplitudes were significantly higher in the subdural strips as compared to the depth electrodes; however, the values were not statistically different between left (n=3) and right (n=4) hemisphere recordings (Figure 2B). The power spectrum did not reveal narrow-band noise in the recordings (Figure 2C). Of 4 subjects, Subject 02's bilateral electrodes were surgically repositioned for suboptimal placement and the repositioning resulted in improved therapeutic effects. The results in this paper focus on the physiological signals after electrodes were repositioned. The types of tics each patient manifested were different, and these subtypes are outlined in Figure 3A with the dominant tic location highlighted in red. Three out of 4 patients had dominant vocal tic and facial tics, 2 out of 4 patients had dominant shoulder and neck tics, and 1 out of 4 patients had dominant hand tics.

DBS Active Contact Localization and Time-Frequency Features of Tic Onset

The placements of the bilateral subdural strips are shown in Figure 3B. All four patients had bilateral subdural strips placed over the hand M1 cortex, and the strips were purposely overlapped in the areas of the premotor and somatosensory cortex. It is noted that the subdural strip over the right hemisphere of Subject 03 was placed more posterior than the other subjects and only the most anterior contact interfaced with the edge of the M1 cortex; therefore, the right hemisphere of Subject 03 was excluded from the analysis when computing the M1 cortex tic feature. The placements of the bilateral CM thalamic depth hand tics. electrodes are shown in Figure 3D. All four subjects were shown to have bilateral depth electrodes placed within the CM thalamic region as defined by the modified digital morphable Schaltenbrand-Bailey atlas.

The time-frequency features of tic onset drawn from the M1 cortex to the CM thalamic region is shown in Figure 3C. The cortical electrode contacts used to analyze the time-frequency features were extracted and highlighted in the figure as orange for each participant. The cortical tic features were more diverse in M1 across subjects compared to CM, partly due to variability in subjects' tics and cortical electrode placement. Cortical beta (12-30Hz) power decrease was identified in 2 of 4 patients (Subject 02 and Subject 03), and a low frequency power increase was identified in 3 of 4 patients (Subject 01, Subject 03, and Subject 04). The beta features were not statistically significant (FDR > 0.01) at a group level analysis (Figure 3C). The thalamic features were conserved across all four subjects. Low frequency (3 – 10Hz) power increase with respect to tic onset was observed in all four subjects while 1 subject had broadband power increases in all frequency bands partly due to sharp evoked potentials observed in CM thalamic regions. The low frequency feature remained statistically significant (FDR < 0.01) after group average analysis (Figure 3E).

The spectrogram of a voluntary movement task was shown in the same manner as a tic spectrogram to contrast their features (Figure 4). Although the center frequency differs, the subdural strip recordings revealed strong beta power decrease among all patients. In addition to the beta power decrease, a subtle low frequency power increase was observed slightly before the onset of movement. Both features were statistically significant (FDR < 0.01). In the depth electrode recordings, some subjects revealed slight low frequency power decrease, but this was not statistically significant (FDR > 0.01). Overall, the depth electrode recordings revealed no significant correlates with voluntary movement. The CM and M1 signals did not yield any coherence during baseline, movement, or tics.

Discussion

In the current study, we recorded and analyzed the neural correlates of human tics in the CM thalamic nucleus and the M1 cortex using a sensing-enabled implanted neurostimulator. The implanted neurostimulator facilitated an investigation of TS physiology outside of the acute intraoperative condition and allowed us to differentiate tic from voluntary movement. The data strongly suggest that LFPs from the CM region but not from M1 can be used to separate tic from voluntary movement. Unique to this study was the acquisition of chronic neural activity from awake behaving humans up to 6 months after surgery, which characterized the physiological underpinnings of human tic and facilitated a differentiation from voluntary

movement. These chronic recordings of thalamic and motor cortical activity provide additional insights into TS pathology and improve upon the limited existing MER and intraoperative LFP recordings [19,33].

Based on previous intraoperative LFP recordings, low frequency power is known to be elevated in TS patients, and such low frequency power is correlated with symptom severity [20]. Given the intermittent nature of TS symptoms, we hypothesized that the low frequency power increase was associated with tic onsets. Our analysis of the tic onset spectrogram confirmed this notion (Figure 3). We identified a strong low frequency (<10Hz) activity that persisted in chronic post-operative LFP recordings in the CM thalamic nucleus. The low frequency activity was time-locked to tic onset and was observable throughout multiple months of chronic recordings. This low frequency power increase and its relationship to tic onset was consistently observed in all subjects (n=4) and resulted in a statistically significant feature after correction for false discovery. To eliminate the possibility of machine interference or motion artifacts causing a low frequency power increase, we performed the same analysis with voluntary movement onset. When the subjects were voluntarily moving and mimicking tics, we observed no statistically significant features in the CM thalamic region. Therefore, we concluded within our cohort that the low frequency power increase was a tic-related feature and was independent from voluntary movement.

Furthermore, the cortical spectrogram across all patients was more diverse than those of the CM thalamus (Figure 3). A broadband beta (12 – 30Hz) power decrease was observed in 2 of 4 subjects, beta power increase was observed in 1 of 4 subjects, and low frequency (<10Hz) power increase was observed in 3 of 4 subjects during tics. These differences in cortical features are limitations possibly due to the placement of the strip and to the diversity of tic morphologies. Figure 3A demonstrates not only that the dominant tics varied between subjects, but the cortical placement also differed. Recordings in the CM thalamic nucleus were more consistent, likely due to its smaller volume. However, one feature that appeared as statistically significant, despite manifesting different tic morphology and recording locations was the low frequency (<10Hz) power increase. The usefulness of that feature was however diminished. Voluntary movement tasks are associated with a low frequency power increase associated with movement onset meaning, that the feature was not tic specific.

One of the limitations of our study was the limited coverage provided by the subdural strips. The 4-contact subdural strip used in the study facilitated recording over a small area of the motor cortex. Tics are often in multiple body regions and the size of our grid could not provide adequate spatial coverage. Prefrontal cortex, in particular, has been a potentially critical location for understanding TS limbic circuitry and tic sensory premonitory urge, however, we did not target this area in this study cohort [34]. Additionally, the depth electrodes were targeted based on pure anatomical mapping using a modified digital morphable Schaltenbrand-Bailey atlas. Functional mapping of the CM thalamic nucleus during DBS surgery has yet to be fully optimized. Finally, the targeting trajectory was selected to avoid damaging blood vessels during DBS lead insertion. Another limitation was the signal quality of the Activa PC+S system. Due to stimulation artifacts generated by therapeutic stimulation, it is difficult to resolve low-frequency signals in thalamic nuclei during stimulation. This limitation prevented us from verifying the above-mentioned tic

features during stimulation and understanding the effect of DBS in the CM thalamic nucleus region as applied for TS patients. Finally, the tic-related feature identified in this study most commonly occurred at, or slightly after, the onset of the tic as opposed to a premonitory urge that occurs prior to tic onset. Responsive stimulation based on this signal may not therefore be detected prior to tic and be used exclusively to stimulate and to prevent tic prior to onset. However, since tics are intermittent and repetitive and occur over an extended period of time, this physiology could still be useful to prevent tic flurries following the initial onset. The improvement in tic, similar to what has been observed in responsive stimulation for epilepsy, seems to be twofold. First, when we observe a signal prior to the tic (the minority of cases), the device can stimulate and suppress it. Second, as the device discharges more times during a 24 hour epoch, there seems to be a normalization of the resonant oscillatory activity. This change in oscillatory activity is associated with less tics. More data will be required to understand and to evaluate the usefulness of this feature for responsive stimulation therapy and how it may potentially improve the therapeutic outcome for TS patients. Collectively, these factors were important limitations to the current study.

This study revealed the thalamic and cortical correlates of tic pathology recorded from human adult TS patients. Recordings from multiple nodes in the human TS network contributed to a better understanding of the phenomenon of human tic. The low frequency power feature in the CM thalamic nucleus region was not a persistent pathological rhythm (such as the beta band observed in Parkinson's disease, or PD [35,36]), but was closely associated with and time-locked to the tic symptoms. The PD literature has shown that delivering stimulation adaptively based on a pathological beta signal can improve many disease related features [37,38]. Delivering stimulation based on the pathological low frequency TS power burst may possibly provide a similar improvement. The tic-onset feature observed in the CM thalamic nucleus region, which can be differentiated from voluntary human movement, is therefore one potential candidate marker for a responsive DBS trial.

Acknowledgements

The authors would like to thank our clinical programmer Pam Zeilman, clinical coordinator Erin Monari, and all involved staff at the University of Florida Fixel Institute for Neurological Diseases for their efforts caring for our participants. The authors would also like to thank the members of Brain Mapping Laboratory for the discussions and comments which were useful in paper preparation.

Funding

This work was supported by grants from the National Institutes of Health R01NS096008 (Okun & Gunduz) and NSF PECASE Award 1553482 (Gunduz). Devices used in this study were donated by Medtronic PLC for investigational purposes only.

References

1. Gilbert D Treatment of Children and Adolescents With Tics and Tourette Syndrome. J Child Neurol 2006;21:690–700. doi:10.1177/08830738060210080401 [PubMed: 16970870]
2. Shapiro E, Shapiro AK, Fulop G, et al. Controlled study of haloperidol, pimozide and placebo for the treatment of Gilles de la Tourette's syndrome. Arch Gen Psychiatry 1989;46:722–30.http://www.ncbi.nlm.nih.gov/pubmed/2665687 (accessed 13 Jun 2018). [PubMed: 2665687]

3. Caine ED, Polinsky RJ, Kartzinel R, et al. The trial use of clozapine for abnormal involuntary movement disorders. Am J Psychiatry 1979;136:317–20. doi:10.1176/ajp.136.3.317 [PubMed: 154301]
4. Piacentini J, Woods DW, Scahill L, et al. Behavior Therapy for Children With Tourette Disorder. JAMA 2010;303:1929. doi:10.1001/jama.2010.607 [PubMed: 20483969]
5. Azrin NH, Peterson AL. Treatment of tourette syndrome by habit reversal: A waiting-list control group comparison. Behav Ther 1990;21:305–18. doi:10.1016/S0005-7894(05)80333-8
6. Schrock LE, Mink JW, Woods DW, et al. Tourette syndrome deep brain stimulation: A review and updated recommendations. Mov Disord 2015;30:448–71. doi:10.1002/mds.26094 [PubMed: 25476818]
7. Visser-Vandewalle V, Temel Y, Boon P, et al. Chronic bilateral thalamic stimulation: a new therapeutic approach in intractable Tourette syndrome. J Neurosurg 2003;99:1094–100. doi:10.3171/jns.2003.99.6.1094 [PubMed: 14705742]
8. Vandewalle V, van der Linden C, Groenewegen H, et al. Stereotactic treatment of Gilles de la Tourette syndrome by high frequency stimulation of thalamus. Lancet 1999;353:724. doi:10.1016/S0140-6736(98)05964-9
9. Worbe Y, Malherbe C, Hartmann A, et al. Functional immaturity of cortico-basal ganglia networks in Gilles de la Tourette syndrome. Brain 2012;135:1937–46. doi:10.1093/brain/aws056 [PubMed: 22434213]
10. Wang Z, Maia TV., Marsh R, et al. The Neural Circuits That Generate Tics in Tourette's Syndrome. Am J Psychiatry 2011;168:1326–37. doi:10.1176/appi.ajp.2011.09111692 [PubMed: 21955933]
11. Caligiore D, Mannella F, Arbib MA, et al. Dysfunctions of the basal ganglia-cerebellar-thalamo-cortical system produce motor tics in Tourette syndrome. PLoS Comput Biol2017;13:e1005395. doi:10.1371/journal.pcbi.1005395 [PubMed: 28358814]
12. Babel TB, Warnke PC, Ostertag CB. Immediate and long term outcome after infrathalamic and thalamic lesioning for intractable Tourette's syndrome. J Neurol Neurosurg Psychiatry 2001;70:666–71. doi:10.1136/JNNP.70.5.666 [PubMed: 11309463]
13. Hassler R, Dieckmann G. [Stereotaxic treatment of tics and inarticulate cries or coprolalia considered as motor obsessional phenomena in Gilles de la Tourette's disease]. Rev Neurol (Paris) 1970;123:89–100.http://www.ncbi.nlm.nih.gov/pubmed/4932913 (accessed 5 Dec 2018). [PubMed: 4932913]
14. Robertson M, Doran M, Trimble M, et al. The treatment of Gilles de la Tourette syndrome by limbic leucotomy. J Neurol Neurosurg Psychiatry 1990;53:691–4.http://www.ncbi.nlm.nih.gov/pubmed/2213047 (accessed 18 Jun 2018). [PubMed: 2213047]
15. McCairn KW, Nagai Y, Hori Y, et al. A Primary Role for Nucleus Accumbens and Related Limbic Network in Vocal Tics. Neuron 2016;89:300–7. doi:10.1016/j.neuron.2015.12.025 [PubMed: 26796690]
16. McCairn KW, Bronfeld M, Belelovsky K, et al. The neurophysiological correlates of motor tics following focal striatal disinhibition. Brain 2009;132:2125–38. doi:10.1093/brain/awp142 [PubMed: 19506070]
17. Worbe Y, Sgambato-Faure V, Epinat J, et al. Towards a primate model of Gilles de la Tourette syndrome: Anatomo-behavioural correlation of disorders induced by striatal dysfunction. Cortex 2013;49:1126–40. doi:10.1016/J.CORTEX.2012.08.020 [PubMed: 23040317]
18. Mink JW. Basal ganglia dysfunction in Tourette's syndrome: a new hypothesis. Pediatr Neurol 2001 ;25:190–8. doi:10.1016/S0887-8994(01)00262-4 [PubMed: 11587872]
19. Marceglia S, Servello D, Foffani G, et al. Thalamic single-unit and local field potential activity in Tourette syndrome. Mov Disord2010;25:300–8. doi:10.1002/mds.22982 [PubMed: 20108375]
20. Neumann W-J, Huebl J, Briicke C, el al. Pallidal and thalamic neural oscillatory patterns in tourette's syndrome. Ann Neurol 2018;84:505–14. doi:10.1002/ana.25311 [PubMed: 30112767]
21. Shute JB, Okun MS, Opri E, et al. Thalamocortical network activity enables chronic tic detection in humans with Tourette syndrome. Neuroimage Clin 2016;12:165–72. doi:10.1016/j.nicl.2016.06.015 [PubMed: 27419067]

22. Ryapolova-Webb E, Afshar P, Stanslaski S, et al. Chronic cortical and electromyographic recordings from a fully implantable device: preclinical experience in a nonhuman primate. J Neural Eng 2014; 11:016009. doi:10.1088/1741-2560/11/1/016009 [PubMed: 24445430]
23. Diagnostic and statistical manual of mental disorders : DSM-5. 5th ed. Arlington, VA: : American Psychiatric Association, 2013 https://searchworks.stanford.edu/view/10157266 (accessed 10 Aug 2017).
24. Foote KD, Okun MS. Ventralis intermedius plus ventralis oralis anterior and posterior deep brain stimulation for posttraumatic Holmes tremor: two leads may be better than one: technical note. Neurosurgery 2005;56:E445; discussion E445.http://www.ncbi.nlm.nih.gov/pubmed/15794849 (accessed 27 Nov 2018). [PubMed: 15794849]
25. Sudhyadhom A, Okun MS, Foote KD, et al. A Three-dimensional Deformable Brain Atlas for DBS Targeting. I. Methodology for Atlas Creation and Artifact Reduction. Open Neuroimag J 2012;6:92–8. doi:10.2174/1874440001206010092 [PubMed: 23091579]
26. Sudhyadhom A, Haq IU, Foote KD, et al. A high resolution and high contrast MRI for differentiation of subcortical structures for DBS targeting: The Fast Gray Matter Acquisition T1 Inversion Recovery (FGATIR). Neuroimage 2009;47:T44–52. doi:10.1016/J.NEUROIMAGE.2009.04.018 [PubMed: 19362595]
27. Hill NJ, Gupta D, Brunner P, et al. Recording Human Electrocorticographic (ECoG) Signals for Neuroscientific Research and Real-time Functional Cortical Mapping. J Vis Exp Published Online First: 26 6 2012. doi:10.3791/3993
28. Ganos C, Rothwell J, Haggard P. Voluntary inhibitory motor control over involuntary tic movements. Mov. Disord. 2018;33:937–46. doi:10.1002/mds.27346 [PubMed: 29508917]
29. Burg JP. Maximum Entropy Spectral Analysis. In: Proceedings of 37th Meeting Oklahoma City: : Society of Exploration Geophysics 1967.
30. Gonçalves SI, de Munck JC, Pouwels PJW, et al. Correlating the alpha rhythm to BOLD using simultaneous EEG/fMRI: Inter-subject variability. Neuroimage 2006;30:203–13. doi:10.1016/J.NEUROIMAGE.2005.09.062 [PubMed: 16290018]
31. Schalk G, McFarland DJ, Hinterberger T, et al. BCI2000: A General-Purpose Brain-Computer Interface (BCI) System. IEEE Trans Biomed Eng 2004;51:1034–43. doi:10.1109/TBME.2004.827072 [PubMed: 15188875]
32. Dale AM, Fischl B, Sereno MI. Cortical Surface-Based Analysis. Neuroimage 1999;9:179–94. doi:10.1006/nimg.1998.0395 [PubMed: 9931268]
33. Bour LJ, Ackermans L, Foncke EMJ, et al. Tic related local field potentials in the thalamus and the effect of deep brain stimulation in Tourette syndrome: Report of three cases. Clin Neurophysiol 2015;126:1578–88. doi:10.1016/j.clinph.2014.10.217 [PubMed: 25435514]
34. Serrien DJ, Orth M, Evans AH, et al. Motor inhibition in patients with Gilles de la Tourette syndrome: functional activation patterns as revealed by EEG coherence. Brain 2004;128:116–25. doi:10.1093/brain/awh318 [PubMed: 15496435]
35. Hammond C, Bergman H, Brown P. Pathological synchronization in Parkinson's disease: networks, models and treatments. Trends Neurosci 2007;30:357–64. doi:10.1016/J.TINS.2007.05.004 [PubMed: 17532060]
36. Quinn EJ, Blumenfeld Z, Velisar A, et al. Beta oscillations in freely moving Parkinson's subjects are attenuated during deep brain stimulation. Mov Disord 2015;30:1750–8. doi:10.1002/mds.26376 [PubMed: 26360123]
37. Little S, Pogosyan A, Neal S, et al. Adaptive deep brain stimulation in advanced Parkinson disease. Ann Neurol 2013;74:449–57. doi:10.1002/ana.23951 [PubMed: 23852650]
38. Little S, Brown P. The functional role of beta oscillations in Parkinson's disease. Parkinsonism Relat Disord2014;20 Suppl 1:S44–8. doi:10.1016/S1353-8020(13)70013-0 [PubMed: 24262186]

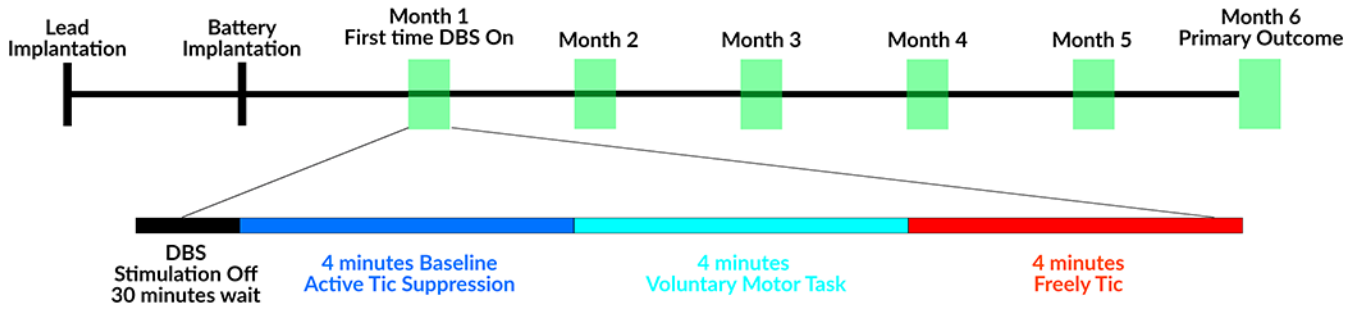

Figure 1. Study timeline.

Recordings were performed in the absence of stimulation, which was turned off at least 30 minutes prior to recording sessions.

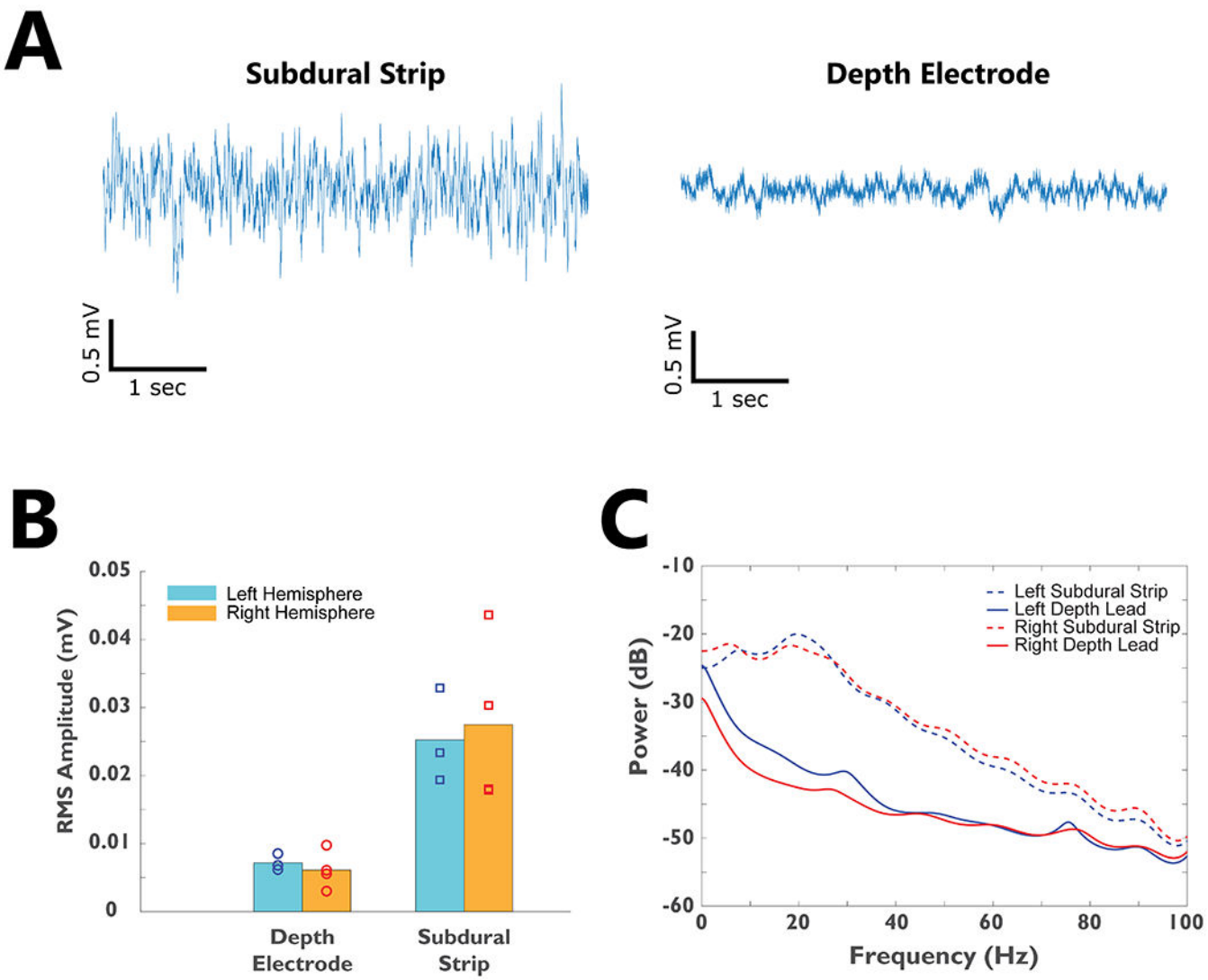

Figure 2. The electrophysiological characteristics of TS subjects recorded using the Medtronic Activa PC+S system.

A)-Raw recordings from the subdural strip and depth electrode implants from a segment of baseline data in one subject. B) The root-mean-square (RMS) amplitude of neural signals recorded from bilateral depth electrodes and subdural strips for all 4 subjects. C) The average power spectrum for all subjects' bilateral subdural strip and depth electrodes.

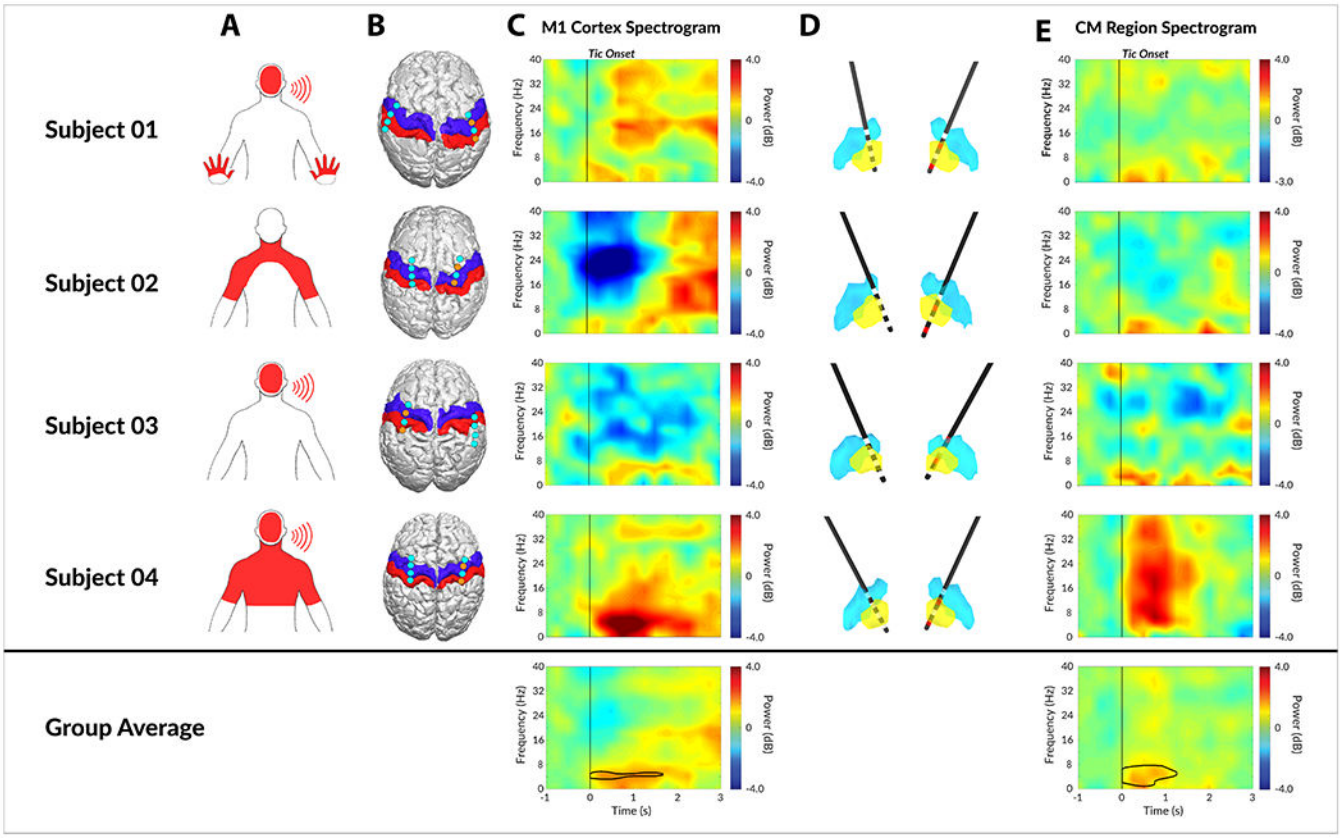

Figure 3. Neural correlates of tic generation in M1 cortex and CM thalamic nucleus.

A) Dominant tic locations as marked on pictograms. B) The localization of bilateral subdural strips from all 4 patients. The blue and red overlay indicate primary motor (M1) cortex and primary somatosensory (S1) cortex respectively. The cyan dots indicate the center of each of the 4 contacts on subdural strips, whereas the orange dots represent bipolar recording electrodes. C) The individual tic onset spectrogram recorded from M1 cortex. D) The localized depth electrodes with digitized atlas. Yellow and blue nuclei represent CM thalamic nucleus and Vim thalamic nucleus respectively. Active contacts for recording are marked in red. E) The individual tic onset spectrogram recorded from CM thalamic nucleus. Area within black contour is statistically significant (FDR < 0.01) in group analysis.

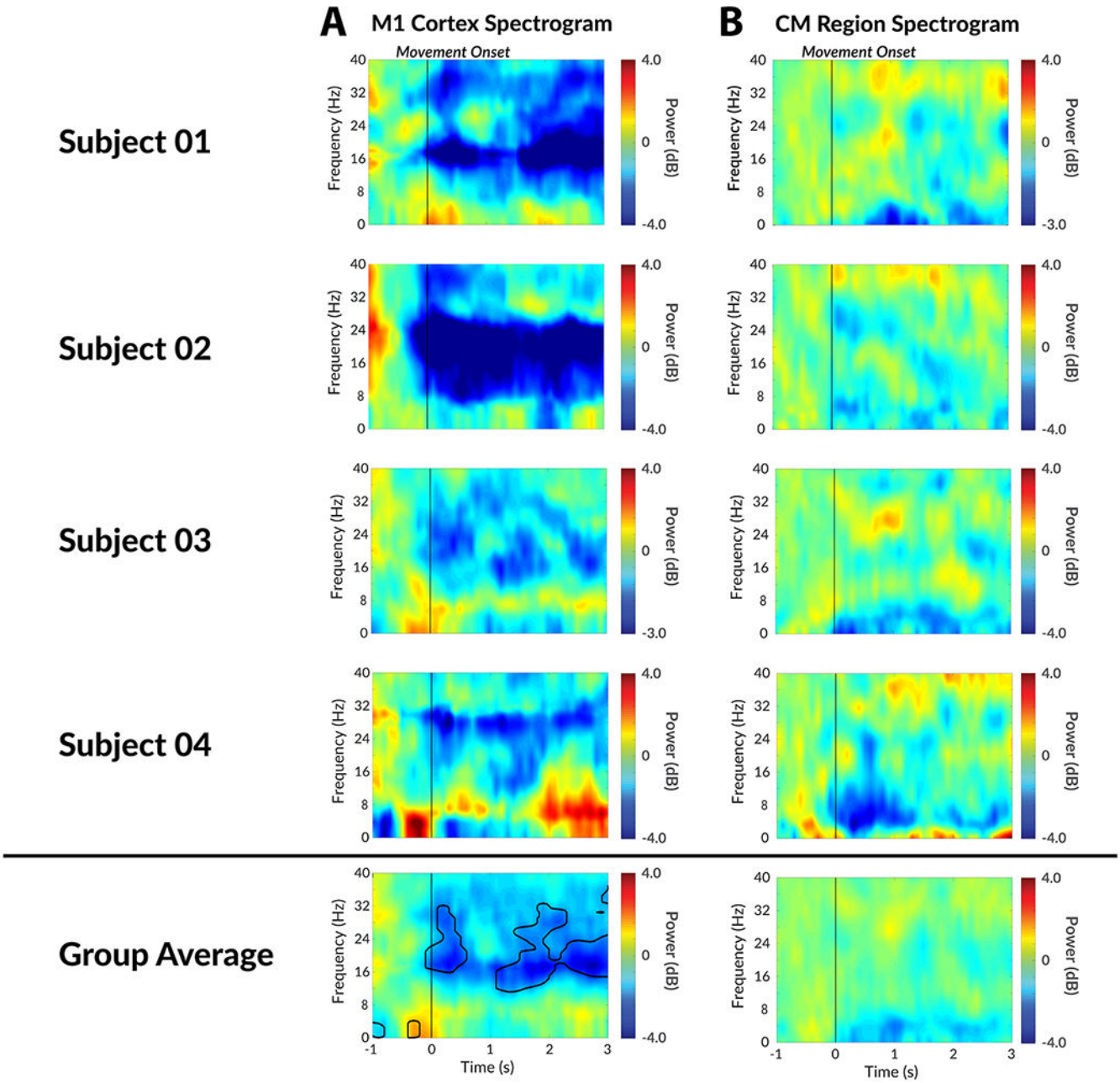

Figure 4. Neural correlates of voluntary movement generation in M1 cortex and CM thalamic nucleus.

A) The individual movement onset spectrogram recorded from M1 cortex. B) The individual movement onset spectrogram recorded from CM thalamic nucleus. Area within black contour is statistically significant (FDR < 0.01) in group analysis.

Table 1.

Subject Baseline Characteristic and Therapeutic Setting

Patient ID	Sex	Age (years)	Disease Duration	MRVRS (tics/min)	YGTSS-Motor	YGTSS-Vocal	Medications at the time of study	Therapeutic Information
TS03	Female	33	16	21-40	22	20	Clonazepam Adderall XR Percocet Prolixin Clonidine	L: E01-CAN, 160Hz, 240uS, 2.9V R: E01-CAN, 160Hz, 240uS, 3.5V
TS04	Male	39	17	21-40	22	20	Zyprexa Paxil CoQ1O	L: E01-CAN, 160Hz, 300uS, 4.0V R: E01-E00, 160Hz, 300uS, 3.5V
TS05	Female	26	20	21-40	22	24	Venlafaxine	L: E02-CAN, 160Hz, 180uS, 4.0V R: E02-CAN, 160Hz, 150uS, 3.5V
TS06	Male	45	34	41-60	23	18	Topiramate	L: E01-CAN, 160Hz, 240uS, 2.5V R: E01-CAN, 160Hz, 240uS. 2.4V

MRVRS: Modified Rush Video Rating Scale

YGTSS: Yale Global Tic Severity Scale